

Empirical validation of network learning with taxi GPS data from Wuhan, China

Susan Jia Xu¹, Qian Xie¹, Joseph Y. J. Chow^{1*}, Xintao Liu²

¹C2SMART University Transportation Center, Dept. Civil & Urban Engineering, New York University, Brooklyn, NY, USA

²Dept. Land Surveying and Geo-informatics, The Hong Kong Polytechnic University, Hong Kong

*Corresponding author: joseph.chow@nyu.edu

ABSTRACT

In prior research, a statistically cheap method was developed to monitor transportation network performance by using only a few groups of agents without having to forecast the population flows. The current study validates this “multi-agent inverse optimization” method using taxi GPS probe data from the city of Wuhan, China. Using a controlled 2062-link network environment and different GPS data processing algorithms, an online monitoring environment is simulated using the real data over a 4-hour period. Results show that using only samples from one OD pair, the multi-agent inverse optimization method can learn network parameters such that forecasted travel times have a 0.23 correlation with the observed travel times. By increasing to monitoring from just two OD pairs, the correlation improves further to 0.56.

Keywords: network learning, multi-agent inverse optimization, taxi trajectory

1. Introduction

Many studies have illustrated the importance to accurately and precisely measure the attributes of an urban transport system. Due to the rise of Big Data and Internet of Things, there are numerous machine learning methods to measure attributes of the transport system. Chow (1) provides an overview of these techniques including several applications like Allahviranloo and Recker (2) for activity pattern prediction; Cai et al. (3) for short-term traffic forecasting; Luque-Baena et al. (4) for vehicle detection; Lv et al. (5) for traffic flow prediction; and Ma et al. (6) for network congestion prediction. However, generic machine learning techniques are not specifically designed to exploit the unique structure of urban transport networks.

As a result, in recent years a theory of inverse problems (see 7) have emerged to capture network structure, dubbed “inverse transportation problems” by Xu et al. (8). If a conventional model M that transforms a set of parameters θ to a set of outputs X as $X = M(\theta)$, then the inverse model deals with estimating the parameters $\hat{\theta}$ based on observed outputs x as $\hat{\theta} = M^{-1}(x)$. Many types of inverse transportation problems have been proposed in the literature: inverse shortest path (9); inverse linear programs for an assortment of transportation problems (10); link capacities in minimum cost flow problems (11); inverse vehicle routing problems (12;13); general inverse variational inequalities for equilibrium models (14); and route choice (15).

Despite the growing literature, inverse transportation problems are designed to take a system level model and estimate parameters of that model from sample data. This is problematic because congested systems require estimation of population attributes like flow in order to quantify congestion effect parameters because the more congested the system the more of an outlier it becomes. Ma et al. (6) is an example of this type of effort, using deep Restricted Boltzmann Machines and Recurrent Neural Networks to estimate population-level flows based on taxi trajectory sample data. Another challenge is the lack of consideration of behavioral mechanisms. Many inference models, particularly those belonging to “network tomography” (see 16; 17), explains the state of the system from the data but do not explain the behavioral mechanisms like route choice on the flow attributes. The system-level inverse transportation problems like Güler and Hamacher (11) result in NP-hard problems that are not scalable to practical size networks.

Xu et al. (8) recently proposed a theory in which the capacity effects of a network are inferred using sampling multi-agent inverse transportation problems instead of solving a single system-level problem. This is possible under the assumption that the agents sampled exhibit behavioral characteristics like route choice preferences. The model infers congested links’ capacity dual variables by using sample of agents’ inverse shortest path problems. A test of the model using queried data from a highway network in Queens, NY, demonstrated the methodology in being able to monitor the network over time and use samples to update the network’s link capacity effects.

In real-world application, obtaining path observations is not always possible. Sometimes the data can be noisy and only contain fragments of actual paths. The contribution of this study is to conduct an empirical study using the methodology from Xu et al. (8) to validate the consistency of the dual variable updates inferred from a taxi sample data set in a real large-size network in Wuhan, China. The method determines travel times in the 2062-link Wuhan network over a four-hour time window. We then display the results of multi-agent IO (MAIO) method for available data, showing that the method provides travel time estimations for an interpretable understanding of network state change in the city. If the methodology works effectively, the estimated travel times based on the inferred dual variables should exhibit a high correlation with the realized travel times of the taxi trajectories. Unlike the Queens, NY, case study in Xu et al. (8), this study would

be the first to validate the inferred dual variables against realized travel times of observed taxi trajectories. Another contribution of this work is the demonstration of using taxi trajectory data to *quantify and explain* the congestion in the network, i.e. not just how congested it is, but how much each link’s congestion impacts the rest of the network (which is more interpretative than methods like 6).

The remainder of the paper is organized as follows. Section 2 reviews studies using taxi trajectory data, and network attributes (i.e. travel time) estimation method, including the methodology from Xu et al. (8). Section 3 presents the experiment design, data preparation, and on-line system simulation set-up steps. The data processing algorithms used in this experiment are introduced in this section. Section 4 discusses the experiment results. Section 5 concludes.

2. Literature review

In a real-world setting, one way to obtain traffic data in a network is from GPS-equipped vehicles. Jenelius and Koutsopoulos (18) called this kind of data as “floating-car” data, where vehicles with GPS equipment installed record their location and speed at fixed time intervals ranging from a few seconds to minutes. As an important component of the urban transport system, taxi offers an all-weather, convenient, comfortable, and personalized travel service for the urban residents, as well as plays a key role in the urban passenger mobility development (19). Taxi GPS trajectories data has been widely used in transportation research, including travel time estimation (20; 21) and travel behavior analysis (22; 23; 24; 25), or for inferring travel momentum in a city (26; 27).

Based on the taxi GPS traces and data mining technology, we can obtain the experienced taxi driver’s route choice behavior in real time and provide guides of shortest path optimal choice for general public (28). There are extensive studies of taxi operations and route choice analysis; however, in this case study, we do not aim at analyzing taxi driver’s practical travel behavior or their activity analysis. The taxi trajectory data is used as sampled heterogeneous agent information to test the MAIO method with a large network.

There are numerous network congestion inference methods using different traffic data. Early efforts in network tomography from Vardi (16) and Tebaldi and West (17) proposed methods to estimate flow distributions from observed link count data. Other studies have sought to integrate route choice behavioral mechanisms in the estimation (29; 30; 31; 32; 33). Deep learning models have been proposed for capturing network congestion (6). System level inverse transportation problems have been proposed to estimate path flows of taxis to have consistent network congestion characteristics (34), who suggested adding a term in the optimization objective function penalizing the travel time between the observation and the sum of link travel times along the path.

The MAIO method from Xu et al. (8) introduces the dual variables in the objective function. The values of dual indicate the change of network state (such as congestion effects) in the form of travel time.

Let us define a network $G(N, A)$ that receives observations from a sample P of agents seeking to travel from an origin node $r_i \in N$ to a destination node $s_i \in N, \forall i \in P$. In the MAIO method, we assume each agent $i \in P$ is rational traversing a network modeled as a capacitated multicommodity problem shown in matrix form in Eq. (1) – (4), where $c_a, a \in A$, is the free flow link cost, x_m is the flow of OD pair $m \in M$, A is the node-link incidence matrix, b_m is $+q_m$ at the source node for OD pair m , $-q_m$ at the sink node, and 0 otherwise. $u_a, a \in A$, is the link capacity.

$$\min_x \sum_m c^T x_m \quad (1)$$

Subject to

$$Ax_m = b_m, \quad \forall m \in M \quad (2)$$

$$\sum_{m \in M} x_m \leq u \quad (3)$$

$$x_m \geq 0, \quad \forall m \in M \quad (4)$$

Solution of this problem can involve a decomposition into a restricted master problem to determine the dual variables w_a corresponding to link capacities u_a . Based on the dual variables, subproblems for each OD pair can then be solved in unbundled form as unconstrained shortest path problems shown in Eq. (5) – (7), where b is a vector of either +1 at the origin, -1, at the destination, and 0 otherwise. The notation ϕ represents the shortest path operator, where ϕ^{-1} is the inverse operator. The dualized link costs are cost \bar{c}_a , i.e. $\bar{c}_a = c_a + w_a$. When there's no congestion, $w_a = 0$. When there is sufficient congestion to cause behavioral change in route choice, $w_a > 0$.

$$\min_y \phi = (c + w)^T y \quad (5)$$

Subject to

$$Ay = b \quad (6)$$

$$y_a \in \{0,1\}, \quad a \in A \quad (7)$$

The MAIO exploits this structure to estimate each agent's perception of w_a , denoted as $w_{a,i}$. In the inverse problem, we observe y_i^* for each agent $i \in P$. If the path chosen is the shortest path according to free flow conditions, then $w_{a,i} \geq 0$ on the path chosen. If another path is chosen, the $w_{a,i}$ for the free flow shorter path needs to be increased. Increasing them optimally to suit each agent is an inverse shortest path problem shown in Eq. (8) – (12) as derived as a linear program from Ahuja and Orlin (35), where v_i are the unbounded node potentials. This problem assumes prior dual variables for each link capacity constraint are available, \bar{w} . The objective is to minimally perturb from the priors to obtain a new dual variable $w_i = \bar{w} - e_i + f_i$ for agent $i \in P$ based on observing their chosen route y_i (Eq. (8)), subject to weak duality (Eq. (9)), strong duality (Eq. (10)), capacity dual variable feasibility (Eq. (11)), and non-negativity constraints (Eq. (12)). $w_i^* = \phi_i^{-1}(g_i, \bar{w}, y_i^*)$ is a function of the OD locations of the agent represented as their graph parameters g_i , the prior, and the chosen path y_i^* .

$$\min_{e_i, f_i, v_i} \phi_i^{-1} = e_i + f_i \quad (8)$$

Subject to

$$A^T v_i \leq c + \bar{w} - e_i + f_i \quad (9)$$

$$b^T v_i = (c + \bar{w} - e_i + f_i)^T y_i^* \quad (10)$$

$$e_i - f_i \leq \bar{w} \quad (11)$$

$$e_i, f_i \geq 0 \quad (12)$$

In an online setting, we assume the population P arrives sequentially over time. In that case, the value of \bar{w} is obtained from a previous agent observation $i - 1$ as $\bar{w} = w_{i-1}^*$ and used to feed a current observation i to update w_i^* . This is summarized in **Algorithm 1**.

Algorithm 1: online learning algorithm to update system capacity dual variables

0. Given: a prior (obtained from a system) $w_0^* = 0$.
1. For each new arrival i ,
 - a. Set $\bar{w} = w_{i-1}^*$.
 - b. Solve an inverse shortest path problem with augmented link costs, $w_i^* = \phi^{-1}(g_i, \bar{w}, x_i^*)$.

Vehicle trajectory data monitoring studies have not yet used the MAIO method from Xu et al. (8) to explain or quantify congestion effects. No tests have been conducted to validate the correlation between output dual variables and real data. A real taxi GPS data set is available. We design an experiment using this data to validate the MAIO methodology.

3. Proposed experiment design

We test the multi-agent IO approach using real taxi data from Wuhan, China. Having observed travel times of the taxis along links, can we demonstrate the existence of correlations with the travel times generated from our monitored link dual variables and the realized travel times under a simulation of an online operation? That is the research question that needs to be addressed by this empirical study. We consider the following criteria to evaluate:

- i. Comparison of the predicted route and the actual route chosen;
- ii. Compute the correlation between real travel times and estimated travel time.

Based on these two criteria, we design an experiment involving multiple time interval observations and evaluate the performance of the MAIO method. Our goal is to show that even with limited OD data, we can see improvement in accuracy of the monitoring system as we go from one OD pair sampling to two OD pair sampling, because additional information will only improve the output.

3.1 Data preparation: network

The data consists of taxi GPS trajectories from Wuhan, China. An urban transport network from Wuhan, China overlaid on OpenStreetMap is shown in **Fig. 1**. The network attributes are available on GitHub: <https://github.com/BUILTNYU/IO-Validation>. Sampled data of free flow link travel times (“FF time”) are presented in **Table 1**. There are 2,833 links and 855 nodes in the extracted urban network. The network is designed to monitor two origin-destination (OD) pairs (see red dots in **Fig. 1**): *Zhongjiacun Station to Wuchang Rail Station*, and *Zhongjiacun Station to Pangxiejia Station*, which are selected from hot spots of pick-ups and drop-offs in the city. The four-hour taxi trajectory data on May 6th, 2014, from 5AM to 9AM, is used for the test.

Algorithms for path reconstruction using GPS coordinates are summarized in **Algorithm 2 – Algorithm 5**. The processed path data, along with the network information and network learning code, are all located in the GitHub site.

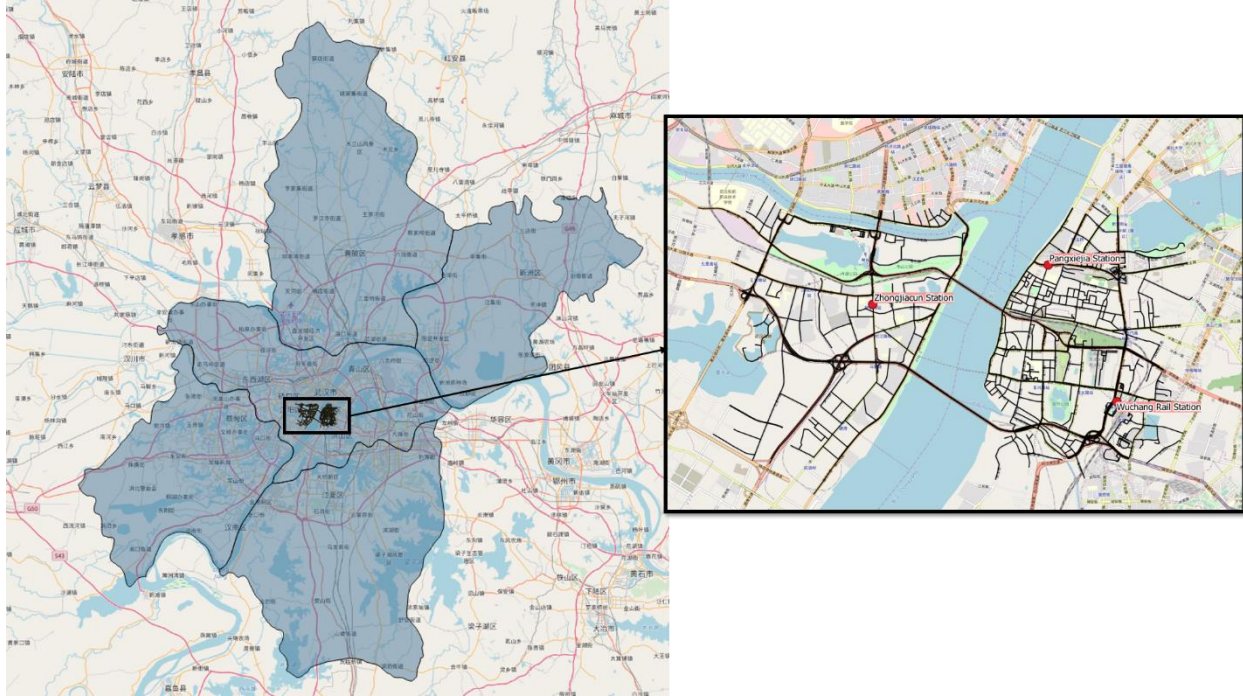


Fig. 1. Study urban transport network in Wuhan, China

Table 1. Sample of link attributes for the study network

Link ID	Start Node ID	End Node ID	Free Flow Time (s)
9	12	1500	16.04
10	12	588	9.34
13	20	1516	7.03
14	20	1504	37.43
15	20	28	5.06
16	22	237	17.09
17	22	1298	14.14
18	22	17	2.66
19	28	20	5.20

3.2 Data preparation: simulation setup

The network is initiated under free flow condition. The multi-agent IO approach keeps updating the travel cost for the whole network every time new path information is obtained (e.g. from the taxi GPS records). When a new path is obtained, we update the effect that the link capacities have on the path using Algorithm 1 such that the observed path is perceived by the agent to be optimal. We monitor and update the system over 4 hours in this case.

The following steps are taken for the experiment.

1. Initiate with values of dual variables equal to zero for all links in the urban transport network in Wuhan, China.
2. Starting at 5:00AM, and every 5 minutes thereafter until 9:00AM,
 - a. For all the trajectories that arrived in that period, identify origin and destination (OD) pairs.
 - b. Run the path reconstruction algorithms (see **Algorithm 2 – Algorithm 5**) to get real-time travelers' choices for each of the OD pairs (in this step, the traveler's choice is assumed as the shortest path).
 - c. Compare the predicted route and the actual route chosen.
 - d. Run **Algorithm 1** to update the link dual variables based on the reconstructed path.
 - e. Compute the correlation between real travel times and estimated travel time.

As congestion occurs in the network, the effects of the capacity on shifting routes (see **Fig. 2** for an illustration of these changes over different time intervals) should be recognized by the network learning algorithm. The dual variables should reflect links that become more congested with binding capacity effects that result in route diversions. The magnitudes of the dual variables should give a relative measure of the insufficient capacity in the link with respect to other links.

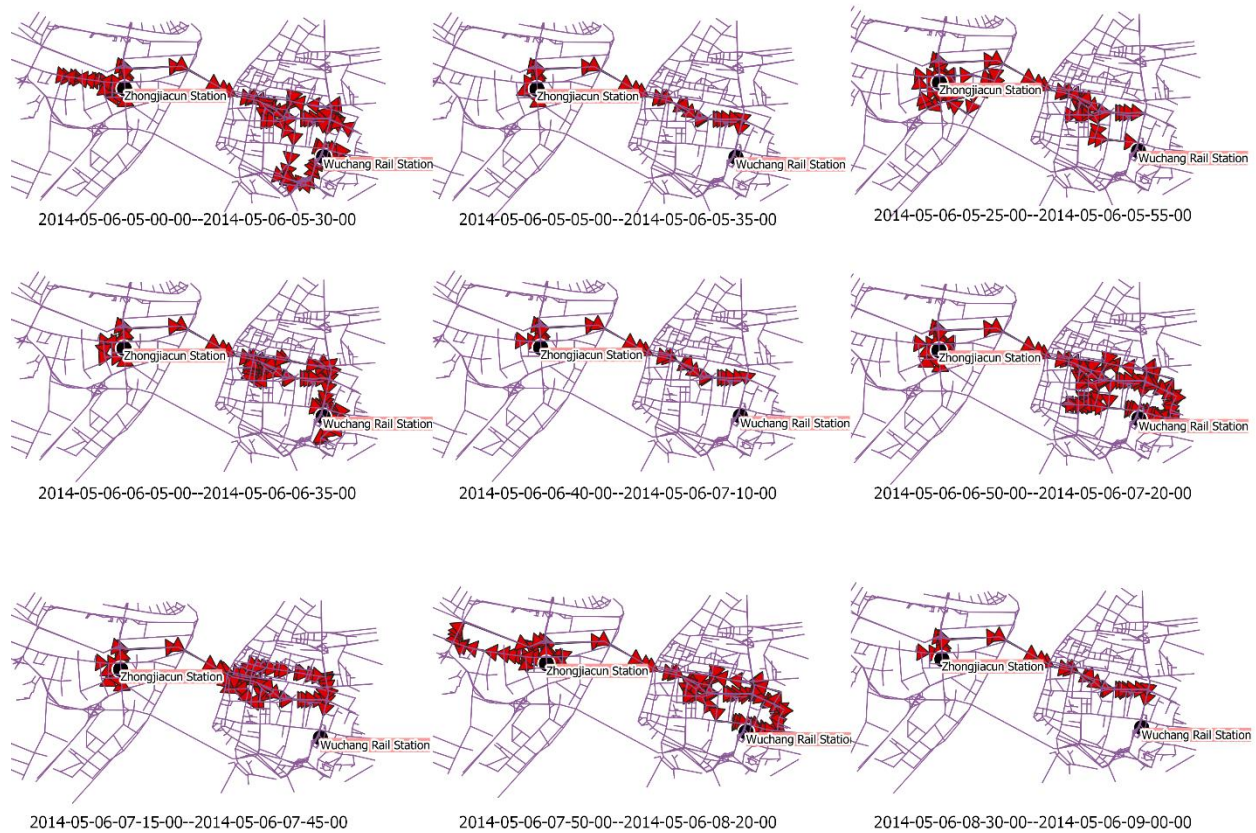


Fig. 2. Sample of route diversions for one OD (from *Zhongjiacun Station* to *Wuchang Rail Station*).

3.3 Data preparation: taxi trajectories

There are about 8,200 taxis operating over 16 hours a day in the city. The dataset used in this test, referred to as the “City of Wuhan Taxi” (COWT) data, contains GPS trajectories of all registered taxis in Wuhan, China. Each GPS entry has information including taxi id, longitude/latitude, time stamp, instantaneous velocity and heading, the operation and occupancy status, as shown in **Table 2**. The minimum interval between two data points is around 15 seconds, and the maximum one is 2 minutes.

Table 1. Sampled data of COWT

ID ¹	Timestamp ²	Longitude	Latitude	Angle ³	Speed ⁴	Operation	Status ⁵
10287	5/4/2014 23:59	114.300472	30.557818	64	20	Operate	0
12448	5/4/2014 23:59	114.137636	30.600324	55	15	Operate	0
4864	5/4/2014 23:59	114.214882	30.571331	94	51	Operate	1
8695	5/4/2014 23:59	114.320283	30.636952	0	0	Operate	0
8538	5/4/2014 23:59	114.298862	30.602568	0	0	Operate	1
2034	5/4/2014 23:59	114.197638	30.558353	0	0	Operate	0
6700	5/4/2014 23:59	114.323372	30.521492	0	1	Operate	0
5620	5/4/2014 23:59	114.415055	30.478973	184	54	Operate	0
10179	5/4/2014 23:59	114.282767	30.612157	190	25	Operate	0

1-ID: Taxi ID; 2-Timestamp: sampling time; 3-Angle: North (0) and South (180); 4-Speed: kilometer per hour;

5-Status: occupied (1) and vacant (0)

The occupancy status associated with each GPS record, which indicates whether there is a passenger in the taxi, is the input to trip segmentation (e.g. the process of dividing taxi trajectories into occupied and vacant trips). A simple rule-based filter can identify unrealistic short occupied trips and fix sudden flips in occupancy status. The processing of taxi trajectories includes the following tasks:

1. GPS points are mapped to the road network based on their coordinates using QGIS
2. Outliers in the trajectory are filtered based on a simple rule, i.e., the speed associated with each GPS points cannot be greater than 120 km/h. Due to the data loss, some taxis have longer time interval between two consecutive GPS points.
3. Trajectories are split into sequences using a time gap threshold of 300 seconds (5-min).

3.4 Data preparation: hotspot identification

Trajectories are split into occupied and vacant trips primarily based on the observed occupancy status. The distribution of trip origins and destinations on the day of May 6th, 2014, is reviewed, and it is expected that pick-ups and drop-offs are more likely to occur in hot spot areas. Hence, heatmaps of taxi pick-ups and drop-offs are created in QGIS 3.4 as shown in **Fig. 3(a)**. The heatmaps show where there is a high concentration of pick-ups and drop-offs, respectively. The hotspots are identified as clusters in **Fig. 3(b)**, which are extracted from the heatmaps. In this case, we select the metro station – *Zhongjiacun* as the origin, and another two metro stations: *Wuchang Rail Station* and *Pengxiejia* as two destinations to have a controlled setting for this experiment.

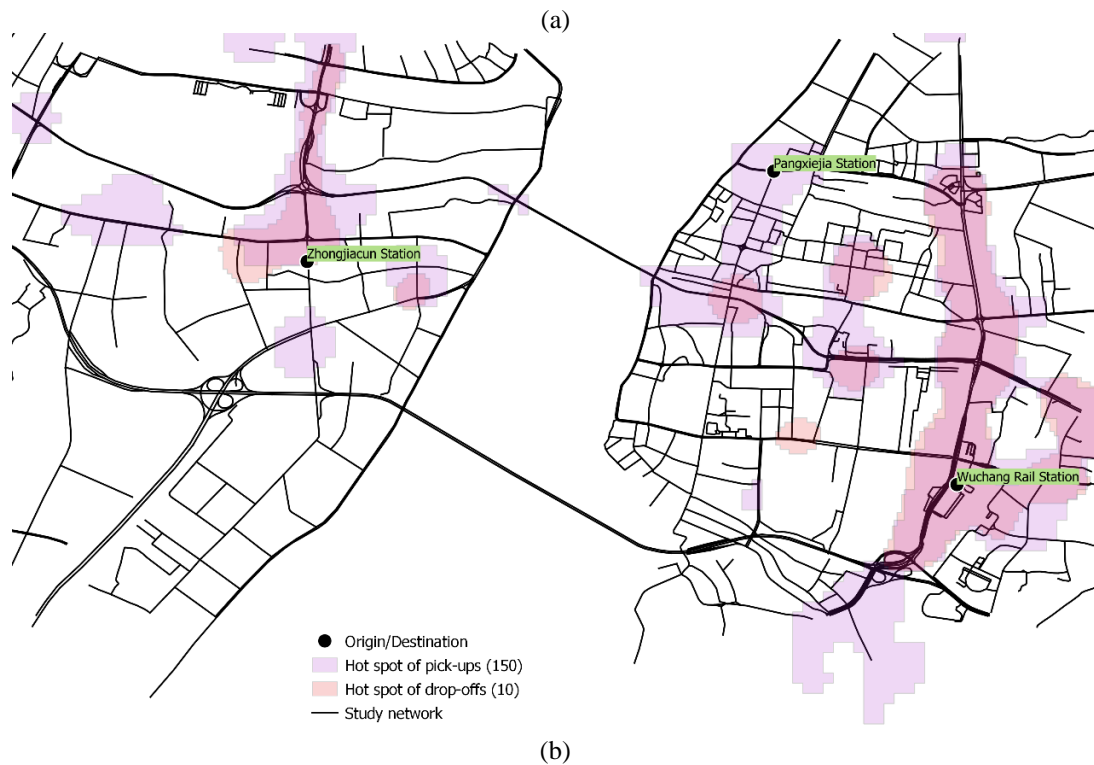
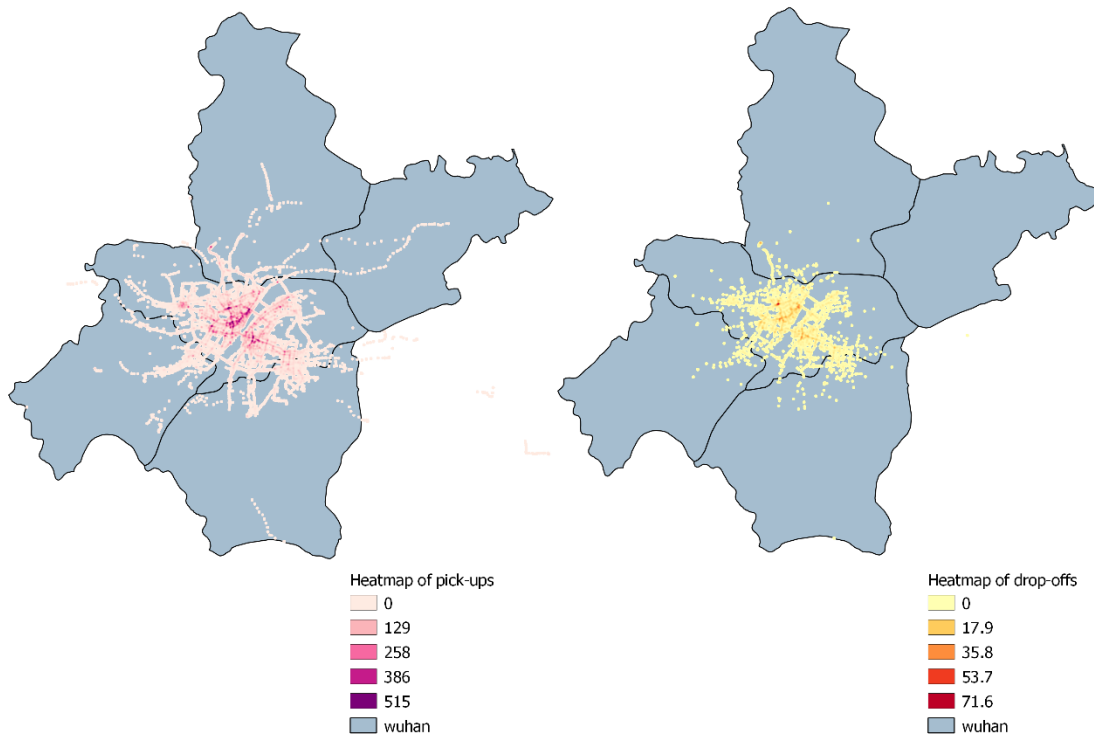


Fig. 3. (a) Heatmaps of taxi pick-ups and drop-offs on May 6th, 2014 in Wuhan, China; (b) Hot spots of taxi pick-ups and drop-offs on May 6th, 2014, and the OD studied in the test

3.5 Data preparation: trip extraction

We define a **trip** as a journey made by a taxi from picking up passengers to dropping off passengers. Since COWT data provides us with the “status” information, we regard a taxi is picking up passengers if the “status” changes from 0 to 1 and dropping off passengers if the “status” changes from 1 to 0. The phrase **trip trajectory** refers to the GPS records generated during part of a trip, which means the status is always 1 in a trip trajectory. Once the OD pair for each experiment is determined, we select those trip trajectories with a starting point close to (within a specific threshold α , say 500 meters) the origin and an ending point close to the destination, as shown in **Algorithm 2**. The following notations used in the algorithms are listed below.

Notation:

O : Origin

D : Destination

E : Set of all directed edges representing real-world roads

G : Directed graph output by Road Network Abstraction algorithm

N : Set of nodes (centroids)

A : Set of arcs (links)

α, β, γ : Proximity thresholds for searching GPS points close to OD, neighboring nodes, and candidate links, respectively

M : One-to-many mapping between node id and node GPS

T : A trip trajectory between the origin and the destination

B : A “best-fit path” including a sequence of links that best fits a GPS trip trajectory

h : Equidistant point (hole) on a road (of a link)

3.6 Data preparation: road network abstraction

The OpenStreetMap shapefile consists of several features and each represents a real-world road fraction with a list of GPS points. We obtain a directed graph by drawing a directed edge from the first GPS point to the last one for each feature. If a feature has a “oneway” attribute B , the corresponding road is bidirectional. Hence, we add an additional directed edge in the opposite direction for such features. Denote the set of all directed edges as E . Each edge has two endpoints and a weight equal to free-flow time calculated as $\frac{length}{maxspeed}$, where the *length* is measured from the feature and the *maxspeed* is an attribute of the feature denoting the speed limit of the road. The missing values of “*maxspeed*” are filled according to the attribute “*fclass*” (tags for identifying the kind of road).

Considering there are many roads with a short length, especially at the crossroads and roundabouts, we remove such roads (edges) by merging the endpoints close to each other, replacing them with a centroid (see **Algorithm 3**). We define “close” by a threshold β , say 50 meters. The output of **Algorithm 3** is a directed graph $G = (N, A)$, where N is the set of the centroids (nodes) and A is the set of arcs.

The main idea of the grid method (see geometric hashing (36)) used to speed up in **Algorithm 3** is to first find the boundary of the road network and divide the network into grids of the same size according to the side length of the boundary, then search for the nearest node in the adjacent grids (with Manhattan Distance not exceeding length along one grid). In the specific implementation, each node has a copy in its 8 adjacent grids. Now the nearest node can be searched

in one grid, which greatly reduces the search time (brute-force approach must traverse all nodes to calculate distances between them).

Algorithm 2 Trip Extraction

Data: Dataframe df contains GPS traces of a taxi, an *origin* and a *destination*

Result: All trip trajectories between origin and destination, allowing deviations within the threshold α

$curCarId = -1$

For each row of records in the dataframe

forall row in df **do**

$carId = row['Car Id']$

if $carId \neq curCarId$ **then**

$inBetween = False$ # True if the point belongs to the sub-trajectory between OD

$pickPassenger = False$ # True if the car picks up a passenger

$havePassenger = False$ # True if the car is serving

$dropPassenger = False$ # True if the car drops off a passenger

end

$p = (row['lon'], row['lat'])$ # a point with longitude and latitude information

if $distance(p, origin) \leq \alpha$ **then**

$inBetween = True$

if $row["status"] == 1$ and not $havePassenger$ **then**

$pickPassenger = True$

end

end

if $distance(p, destination) \leq \alpha$ **then**

$inBetween = True$

if $row["status"] == 1$ and $havePassenger$ **then**

$dropPassenger = True$

end

end

if $dropPassenger$ **then**

 finish reconstructing route

 record the route information

end

if $inRoad$ and $pickPassenger$ **then**

$havePassenger = True$

 start reconstructing route

$takePassenger = False$

 continue

end

if $havePassenger$ **then**

 continue reconstructing route

end

end

Algorithm 3 Road Network Abstraction

Data: $E = \{e \mid e = (point_1, point_2)\}$ contains all edges data. Each edge contains two endpoints and each endpoint contains GPS (lat and lot) information.

Result: Output a graph $G = (N, A)$ representing E . We merge those endpoints whose distances between each other are less than specific threshold β (say 30 meters) to a node in A .

Let $M = \{\}$ be a one-to-many mapping between node id and node GPS.

Let $N = \{\}$, $A = \{\}$ be the set of nodes and arcs.

$i = 1$;

forall $e = (point_1, point_2) \in E$ **do**

NearestNode returns the id of nearest node in M

 # Note that the brute-force approach to implement *NearestNode* runs in $O(E^2)$ time, hence we use the grid method to speedup

$n = \text{NearestNode}(point_1, M)$; $n_1 = n$

forall $p \in M[n]$ **do**

if $\text{distance}(p, point_1) > \beta$ **then**

$n_1 = i$; $i = i + 1$;

$N = N \cup n_1$;

$M = M \cup \{(n_1, point_1)\}$;

break;

end

end

if $n_1 == n$ **then**

$M = M \cup \{(n_1, point_1)\}$;

end

$n = \text{NearestNode}(point_2, M)$; $n_2 = n$

forall $p \in M[n]$ **do**

if $\text{distance}(p, point_2) > \beta$ **then**

$n_2 = i$; $i = i + 1$;

$N = N \cup \{n_2\}$;

$M = M \cup \{(n_2, point_2)\}$;

break;

end

end

if $n_2 == n$ **then**

$M = M \cup \{(n_2, point_2)\}$;

end

if $(n_1, n_2) \notin A$ **then**

$A = A \cup \{(n_1, n_2)\}$;

end

end

3.7 Data preparation: best-fit path

The critical step in the simulation is to reconstruct the actual path of a taxi based on its GPS trip trajectory. However, given OD pairs on the directed graph, there are multiple candidate paths

starting from the origin and ending with the destination, even if the nodes and links are not allowed to be accessed repeatedly. To select an optimal path among the candidate paths, we give the definition of the "best-fit path" here.

Definition 3.1 Given a directed graph $G(N, A)$ and a trip trajectory $T = [p_1, p_2, \dots, p_m]$ of GPS points, where A consists of links representing real-world roads on the map. Each p_i is an observed GPS point containing longitude and latitude information. Let $t(a)$ be the tail of link a and $h(a)$ be the head, and c_a is the length of link a . A "best-fit path" $B = \{a_1, a_2, \dots, a_k\}$ ($a_i \in A$) is a minimum length directed path $\operatorname{argmin}_B \sum_{a \in B} c_a : \{h(a_i) = t(a_{i+1}) \forall i = 1 \dots k - 1; \exists j = 1, \dots, k: d(p_i, a_j) \leq \gamma \forall i = 1, \dots, m - 1\}$. Here $d(p, a)$ is the projection distance between point p and link a , γ is a pre-defined threshold.

Considering 1) the potential GPS errors that bring troubles to the search of "best-fit path" and 2) relatively large time intervals between adjacent GPS records that can lead to many possible paths, we base our path reconstruction algorithms on two assumptions:

- 1) GPS errors do not exceed the threshold γ .
- 2) As a rational man, a taxi driver often locally chooses the shortest path (between the moments when adjacent GPSs are collected).

3.8 Data preparation: path reconstruction

There are some difficulties with path reconstruction. First, the GPS points have certain inaccuracies. It's hard to tell which road a taxi is on, simply return the nearest link may not always be correct. Consider the following three cases: 1) the taxi is on a bidirectional road, the brute-force approach returns the link with opposite direction to the correct one; 2) there is a highway right above a road, the brute-force approach returns the highway when the taxi is actually on the road or the other way around; 3) the taxi is close to the intersection of two roads, the brute-force approach returns the link intersected with the correct one. Second, even if we can decide the road information of two consecutive GPS points, the two roads may be disjoint because the interval between the two data points may be long enough to pass multiple roads (it may take only 20 seconds to pass a block). We need to do data imputation. For example, when a taxi is crossing the Wuhan Yangtze River Tunnel, there is no GPS record due to the bad signal. However, we can use the last GPS record before entering the tunnel and the first one after exiting the tunnel to inference the missing roads (tunnel). Last, we must select the best-fit path from several possible paths for a GPS trajectory.

Considering the first difficulty, we find several link (arc) candidates for each point on a trip trajectory (see **Algorithm 3**). As for the second difficulty, each time we obtain link candidate sets X and Y of adjacent GPS, for each head x in X and for each tail y in Y , we find the shortest path from x to y using Dijkstra's algorithm (see **Algorithm 4**). Since the maximum time interval is just 2 minutes, we consider the shortest path algorithm is reliable to fill in only a few missing toads. Now with several possible paths for a GPS trajectory, we choose the shortest one as the best-fit path (see **Algorithm 5**).

Two steps can be time-consuming. The first is to find candidate links. The brute-force approach searches for real-world roads corresponding to all arcs in the directed graph and calculates the projection distance between each GPS point and each road. The second is that we need to traverse not only all candidate link sets, but also all candidate links in each set, and repeatedly call Dijkstra's algorithm for each combination of candidate links. For the former, we

consider drilling equidistant holes for each road and then searching for the road where the nearest hole is located. In this way, we no longer need to calculate the projection distance between a point and a curve (road), but the Euclidean distance between a point and a point instead. Here we also use the grid method mentioned above to speed-up. The only difference is that if nothing returns after searching the grid and the 8 adjacent grids, we continue searching the grids in outer layers (8i grids on the i^{th} layer) until reaching a specific threshold (say 6^{th} level). For the latter, we also apply some speed-up methods: 1) using tree data structures and dynamic programming; 2) merging duplicate segments of candidate paths.

Algorithm 4 Get Link Candidates

Data: M is a one-to-many mapping between node id and node GPS. $G = (N, A)$ contains nodes and arcs of the whole graph. $T = [p_1, p_2, \dots, p_m]$ is a trip trajectory (series of GPS points) of a vehicle. Each p_i contains longitude and latitude information.

Result: Output a sequence of candidate link sets $S = [C_1, C_2, \dots, C_m]$. Each C_i is a set of candidate link where each link has GPS p_i . We say link a has p_i if p_i is close to a (within threshold γ).

Let $S = []$ be the sequence result.

PunchLine returns a mapping M' between link id and hole GPS

A hole is one of the equidistant points (including endpoints) on the road represented by a link
 $M' = \text{PunchLine}(M, G)$

forall $p \in T$ **do**

 # *NearestHole* returns the link id and hole GPS of the nearest hole in M'

$(a, h) = \text{NearestHole}(p, M')$;

if $\text{distance}(h, p) < \gamma$ **then**

 # *GetallLinks* returns all links if there exists a hole of the link such that the distance between the hole and p is less than the threshold γ

 # Note that the brute-force approach to implement *GetallLinks* runs in $O(PE)$ time, here we also use the grid method to speedup

$C = \text{GetallLinks}(p, M', \gamma)$;

end

else

$C = \{a\}$;

end

 Append C to S ;

end

Algorithm 5 Get Best-fit Path

Data: $G = (N, A)$ contains nodes and arcs of the whole graph, $S = [C_1, C_2, \dots, C_m]$ is the sequence of candidate link sets, where $C_i = \{a_{i1}, a_{i2}, \dots\}$ is the candidate link set of GPS p_i .

Result: Output best-fit path $B = (n_1, n_2, \dots, n_{k+1})$ passing T where each $n_i \in N$ is a node.

for $i \in [1, m]$ **do**

 Let $C'_i = \{n \mid n \in A[a], a \in C_i\}$ be the set of endpoints (nodes) of all links in C_i

end

Let $S_R = \{\}$ be the set of all possible paths

forall $n \in C'_1$ **do**

$B = (n)$; # construct a new path with starting node n

$S_B = S_B \cup \{B\}$ # add new path B to S_B

end

$i = 2$;

while $i \leq m$ **do**

$S'_B = \{\}$ # S'_B is the new possible path

forall $n \in C'_i$ **do**

forall $B \in S_B$ **do**

 # $B = (n_1, n_2, \dots, n_j)$ is the current path

 # get the shortest path B_s from n_j to n with the knowledge B

$B_s = \text{Shortest}(n_j, n, B)$;

 record new $B' = B \parallel B_s$ # get the shortest path B' ending with n

end

$S'_B = S'_B \cup B'$

end

$S_B = S'_B$ # the set of all possible paths that end with points in C'_i

$i = i + 1$

end

return the shortest path in S_B

The experiment parameters are summarized in **Table 3**.

Table 3. Summary of experiment parameters

Number of nodes	855
Number of links	2833
Observation period	from 5AM to 9AM on May 6 th , 2014
Average time between observations	5 minutes
Number of time intervals	48
Number of samples observed for OD 1	132
Number of samples observed for OD 2	48
Number of difference path taken for OD 1	53
Number of difference path taken for OD 2	29
Average observed path travel time/free flow travel time ratio	2.72

A plot of the observed path travel time/free flow travel time ratio over the 180 samples is shown in Fig. 4.

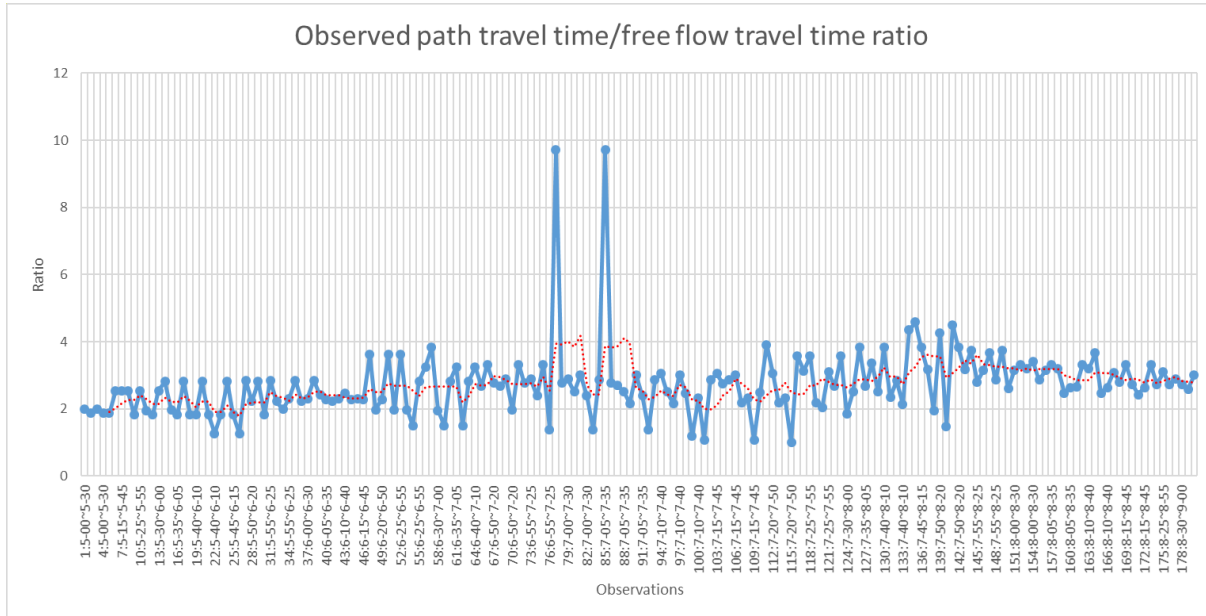


Fig. 4. The observed path travel time/free flow travel time ratio over 180 observed routes from 2 OD pairs

The next section provides the results of monitoring with the MAIO method and comparison of estimated trip travel times using the inferred capacity dual variables w_i^* to the observed travel times.

4. Results

4.1 Simulation of online monitoring

We start with a single OD pair (OD 1: *Zhongjiacun Station* to *Wuchang Rail Station*). The MAIO method is implemented in MATLAB R2017a calling the IBM ILOG CPLEX Optimization Studio v12.8 to solve the inverse shortest path problem in Eq. (8) – (12).

Fig. 5(a) shows the trajectory of the link dual variables (the ones that became binding) as they evolve from one new observation update to the next. The figure illustrates the sensitivity of the method to changes in the network parameters over time, based on the 132 observed individual route choices. There are 409 links traversed by taxis from *Zhongjiacun Station* to *Wuchang Rail Station* in the morning from 5:00 AM to 9:00 AM, and dual variables are positive on 25 links. Those links are highlighted in red in the map, and ones with higher dual variables are labeled.

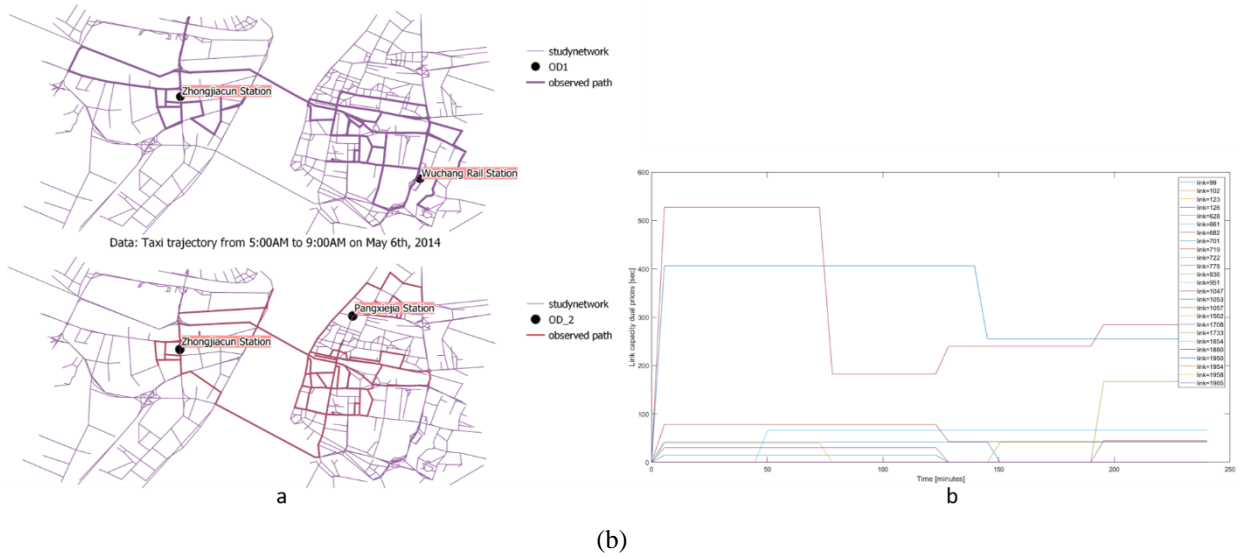
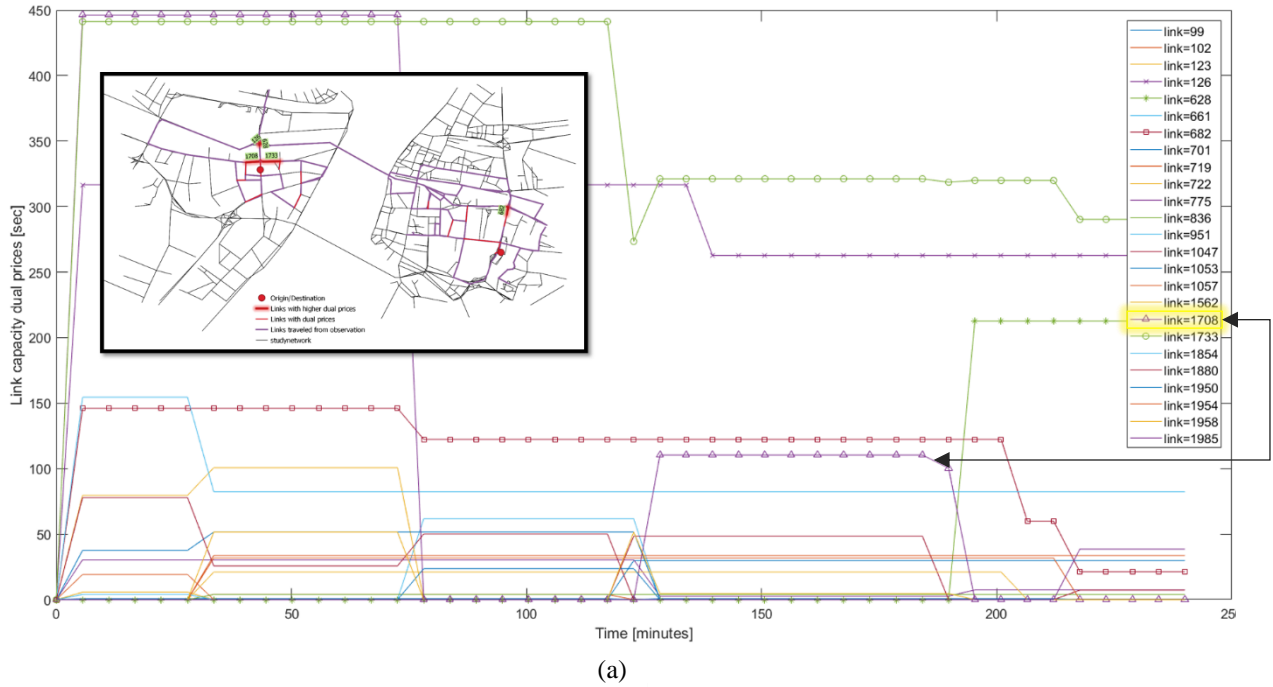


Fig. 5. (a) Trajectories of link dual variables as estimated using Algorithm 2.1 for study network over a 4-hour period; (b) Updated dual variables from new observations as new OD added in the network.

If this result was true, it suggests that link 1708 (road segment near the transport corridor) has the highest dual variable (i.e. 446 sec) before 6:35AM, which means that the link 1708 was the most congested before the congestion was eliminated between 6:35AM and 7:25AM. Then there is a light delay at 110 seconds, and it is not back to 0 again until 7:55AM. This suggests there was an incident in the earlier spike as it was not sustained. On the other hand, link 1733 has a sustained congestion throughout the whole period, suggesting heavy usage under recurrent congestion effect. These results confirm the method from Xu et al. (8) in being able to estimate dual variables (or congestion effects) in real-world urban network that can provide interpretable insights to a decision-maker.

What happens if we sampled from multiple OD paths instead of just one (changing our sampling frame)? We add one more OD pair to observations (OD 2: 48) and re-run the experiment to see how the network state changes. The temporal profile of link dual variables looks quite different. The observed links are mapped on the left in **Fig. 5(b)**, while the link dual variables are updated as shown in the profile on the right of **Fig. 5(b)**. The dual variable for link 1708 drops significantly as compared to the one from monitoring a single OD only. This demonstrates that the effectiveness of the MAIO method depends on effective sampling across different OD pairs to provide more comprehensive coverage over the network. Focusing only on data from a limited set of OD pairs can limit the correctness of the magnitude. As more route observations over different parts of the network are considered, they provide more information about the dual variables, which changes the magnitudes of the other paths that overlap. Ideally, every OD pair should be sampled, but this may not always be possible.

4.2 Correlation between observed travel times and online monitoring

Finally, we include a comparison between real travel times and estimated travel times to show the accuracy improvement on estimation. We understand that this is data drawn *only* from two OD pairs, so we do not expect a complete picture. Rather, we want to demonstrate that even with only two OD pair sampling, we can achieve some accuracy in the monitoring for the whole network and this improves upon the accuracy achieved with only one OD pair sampling.

Fig. 6 shows similarities between estimated travel times (i.e. free flow travel time plus estimated dual variables on traveled links) and real travel times (i.e. the time stamp of last GPS points minus the first in each trip segment) for all observed route choices. There are 180 observations in total, of which 48 observations are from the new OD.

We can draw two conclusions. First, graphically estimations based on the MAIO method using two OD sampling is clearly more accurate than using only one OD sampling. Second, when we compute the correlations between the observed and estimated travel times, we see that the correlation value for the single OD and two OD pairs are 0.23 and 0.56, respectively. This provides validity that using only samples from only two OD pairs we can get a good picture of the actual network, and it improves significantly (more than doubling the correlation) from one OD pair sampling. This suggests that the MAIO method can provide a good fit to the true observations. This is a statistically cheap method as it does not require forecasting population flows.

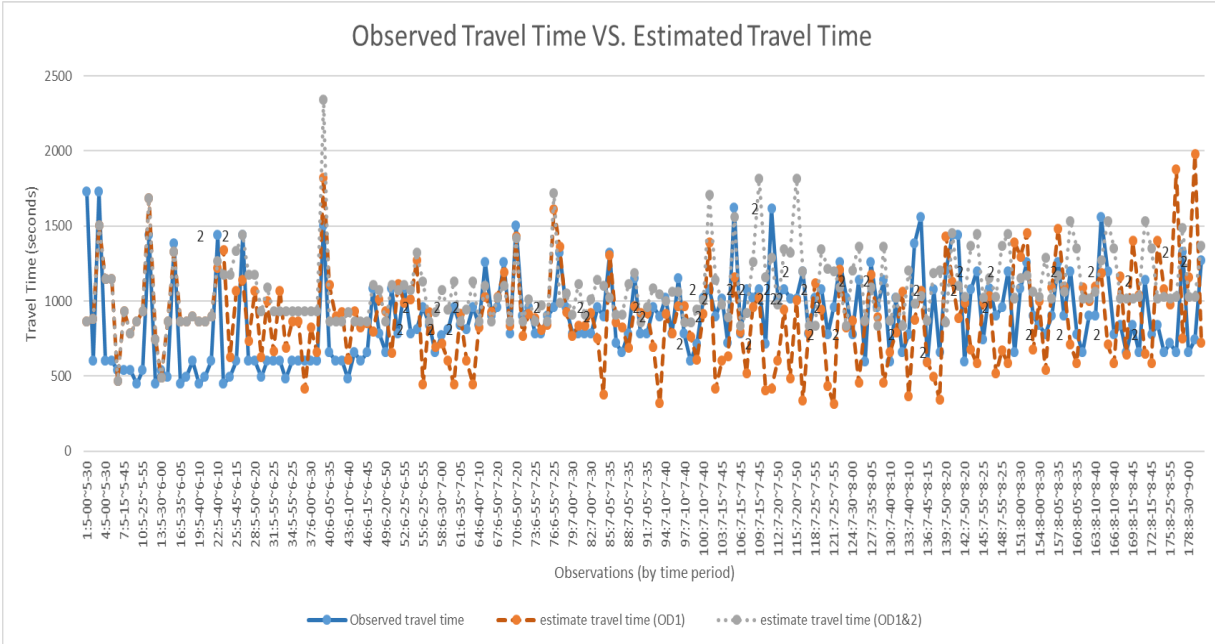


Fig. 6. Estimated travel times and real travel times for 180 observed routes from single and two OD pairs

5. Conclusion

The proposed MAIO model in Xu et al. (8) infers capacity effects throughout a network using only GPS probe samples without the statistically costly step of forecasting population flows. However, the earlier study only provided a theoretical argument and numerical illustration using real data. No validation of the accuracy of the method in monitoring a system is provided. We address this research gap by applying the MAIO method to taxi GPS data in a controlled network setting to simulate an online environment.

Several conclusions are drawn from this empirical validation experiment. Network system attributes like link capacity dual variables can be updated using only samples of individual route observations (e.g., taxi GPS trajectories), without estimating the total link or path flows. This demonstrates that the MAIO method can cheaply monitor a transportation network’s system performance over time. The dual variable changes show that the inferences model is indeed sensitive to changes in the system. As traffic increases from 5:00 AM to 9:00 AM in the study period resulting in more spillbacks and incidents impacting link capacities, the set of dual variables steadily increases on average, as shown in **Fig. 5**. The accuracy of the inference is illustrated by the correlation between observed travel time and estimated travel times based on the dual variables updated from the MAIO method. The visual comparison (see **Fig. 6**) indicates the similarities and how they improve after sampling from one OD pair to two. The higher value of correlation for 2 OD pairs shows that the multi-agent IO method performs well in estimating dual variables (or congestion effects) in the form of travel time, and more observations from other OD pairs will only enhance the model performance.

One of the major difficulties in this paper is data processing, that is, how to extract and reconstruct the best-fit paths from raw taxi GPS trajectories. Both GPS errors and the lack of information caused by the large interval between adjacent GPS need to be considered. The path reconstruction process is performed by implementing several algorithms: trip extraction algorithm

obtaining trajectories that meet the requirement of our experiments, the road network abstraction algorithm converting the complex map into a directed graph, the candidate edge algorithm finding candidate edges for each GPS points, and the best-fit path selection algorithm applying various pruning techniques and acceleration techniques to efficiently select the best-fit path from a large number of candidate paths for each trajectory.

Future work should implement this system in a real-world setting using GIS tools and use the monitoring with predefined thresholds to set alerts for dual variables in an online dashboard. Related work can also include monitoring a network before, during, and after a disaster to quantify the impact of dual price increases due to capacity degradation. Since user GPS data may not be freely shared due to privacy concerns, we may experiment with using a blockchain design to anonymize GPS data shared by users or setting up a differential privacy-oriented database (1).

Acknowledgements

This study was conducted with support from the NSF CAREER grant, CMMI-1652735. One of the authors (Xintao Liu) was supported by The Hong Kong Polytechnic University Start-up Research Fund Program: [Grant Number 1-ZE6P]; Area of Excellence: [Grant Number 1-ZE24].

References

1. Chow, J. Y. J. (2018). *Informed Urban Transport Systems: Classic and Emerging Mobility Methods Toward Smart Cities*. Elsevier
2. Allahviranloo, M., & Recker, W. (2013). Daily activity pattern recognition by using support vector machines with multiple classes. *Transportation Research Part B: Methodological*, 58, 16-43.
3. Cai, P., Wang, Y., Lu, G., Chen, P., Ding, C., & Sun, J. (2016). A spatiotemporal correlative k-nearest neighbor model for short-term traffic multistep forecasting. *Transportation Research Part C: Emerging Technologies*, 62, 21-34.
4. Luque-Baena, R. M., López-Rubio, E., Domínguez, E., Palomo, E. J., & Jerez, J. M. (2015). A self-organizing map to improve vehicle detection in flow monitoring systems. *Soft Computing*, 19(9), 2499-2509.
5. Lv, Y., Duan, Y., Kang, W., Li, Z., & Wang, F. Y. (2014). Traffic flow prediction with big data: a deep learning approach. *IEEE Transactions on Intelligent Transportation Systems*, 16(2), 865-873.
6. Ma, X., Yu, H., Wang, Y., & Wang, Y. (2015). Large-scale transportation network congestion evolution prediction using deep learning theory. *PloS one*, 10(3), e0119044.
7. Tarantola, A. (2005). *Inverse problem theory and methods for model parameter estimation* (Vol. 89). siam.
8. Xu, S. J., Nourinejad, M., Lai, X., & Chow, J. Y. J. (2018). Network learning via multiagent inverse transportation problems. *Transportation Science*, 52(6), 1347-1364.
9. Burton, D., & Toint, P. L. (1992). On an instance of the inverse shortest paths problem. *Mathematical Programming*, 53(1-3), 45-61.
10. Ahuja, R. K., & Orlin, J. B. (2001). Inverse optimization. *Operations Research*, 49(5), 771-783.
11. Güler, Ç., & Hamacher, H. W. (2010). Capacity inverse minimum cost flow problem. *Journal of Combinatorial Optimization*, 19(1), 43-59.
12. Chow, J. Y. J., & Recker, W. W. (2012). Inverse optimization with endogenous arrival time constraints to calibrate the household activity pattern problem. *Transportation Research Part B: Methodological*, 46(3), 463-479.
13. You, S. I., Chow, J. Y. J., & Ritchie, S. G. (2016). Inverse vehicle routing for activity-based urban freight forecast modeling and city logistics. *Transportmetrica A: Transport Science*, 12(7), 650-673.
14. Bertsimas, D., Gupta, V., & Paschalidis, I. C. (2015). Data-driven estimation in equilibrium using inverse optimization. *Mathematical Programming*, 153(2), 595-633.

15. Hong, S. P., min Kim, K., Byeon, G., & Min, Y. H. (2017). A method to directly derive taste heterogeneity of travellers' route choice in public transport from observed routes. *Transportation Research Part B* 95, 41-52.
16. Vardi, Y. (1996). Network tomography: Estimating source-destination traffic intensities from link data. *Journal of the American statistical association*, 91(433), 365-377.
17. Tebaldi, C., & West, M. (1998). Bayesian inference on network traffic using link count data. *Journal of the American Statistical Association*, 93(442), 557-573.
18. Jenelius, E. and Koutsopoulos, H. N. (2013) Travel time estimation for urban road networks using low frequency probe vehicle data. *Transportation Research Part B* 53, 64-81.
19. Han S.S. (2010). Managing motorization in sustainable transport planning: the Singapore experience. *Journal of Transport Geography*, vol. 18, no. 2, 314–321.
20. Hoeitner, A., Herrin, R., Abbeel, P., Bayen, A. (2012). Learning the dynamics of arterial traffic from probe data using a dynamic bayesian network. *IEEE Transactions on Intelligent Transportation Systems* 13(4): 1679-1693.
21. Wang, Y., Zheng, Y., Xue, Y. (2014). Travel time estimation of a path using sparse trajectories. *Proceedings of the 20th ACM SIGKDD International Conference on Knowledge Discovery and Data Mining*, 25-34 (KDD 2014)
22. Hi, X., An, S., and Wang, J. (2014). Exploring urban taxi drivers' activity distribution based on GPS data. *Mathematical Problems in Engineering*, 2, 1-13.
23. Jiang, B., Yin, J., Zhao, S. (2009) Characterizing the human mobility pattern in a large street network. *Phys Rev E* 80(2):021136.
24. Liu, L., Andris, C., and Ratti, C. (2010). Uncovering cabdrivers' behavior patterns from their digital traces. *Computers, Environment and Urban Systems*, vol. 34, no. 6, 541–548.
25. Zhao, P., Liu, X., Kwan, M.P. and Shi, W. (2018). Unveiling cabdrivers' dining behavior patterns for site selection of "taxi Canteen" using taxi trajectory data. *Transportmetrica A: Transport Science*, 1-24.
26. Liu, X., Chow, J. Y. J., & Li, S. (2018). Online monitoring of local taxi travel momentum and congestion effects using projections of taxi GPS-based vector fields. *Journal of Geographical Systems*, 20(3), 253-274.
27. Shen, J., Liu, X., & Chen, M. (2017). Discovering spatial and temporal patterns from taxi-based Floating Car Data: a case study from Nanjing. *GIScience & Remote Sensing*, 54(5), 617-638.
28. Zheng, Y., Yuan, J., Xie, W., Xie, X., and Sun, G. (2010). Drive smartly as a taxi driver. in *Proceedings of the Symposia and Workshops on Ubiquitous, Autonomic and Trusted Computing (UIC-ATC '10)*, 484–486, IEEE Computer Society.
29. Srinivasan, K. K., & Mahmassani, H. S. (2000). Modeling inertia and compliance mechanisms in route choice behavior under real-time information. *Transportation Research Record*, 1725(1), 45-53.
30. Dia, H. (2002). An agent-based approach to modelling driver route choice behaviour under the influence of real-time information. *Transportation Research Part C: Emerging Technologies*, 10(5-6), 331-349.
31. Frejinger, E., & Bierlaire, M. (2007). Capturing correlation with subnetworks in route choice models. *Transportation Research Part B: Methodological*, 41(3), 363-378.
32. Ben-Elia, E., & Shiftan, Y. (2010). Which road do I take? A learning-based model of route-choice behavior with real-time information. *Transportation Research Part A: Policy and Practice*, 44(4), 249-264.
33. Gao, S. (2012). Modeling strategic route choice and real-time information impacts in stochastic and time-dependent networks. *IEEE Transactions on Intelligent Transportation Systems*, 13(3), 1298-1311.
34. Bertsimas, D., Delarue, A., Jaillet, P., & Martin, S. (2019). Travel Time Estimation in the Age of Big Data. *Operations Research*, 67(2), 498-515.
35. Ahuja, R. K., & Orlin, J. B. (2001). Inverse optimization. *Operations Research*, 49(5), 771-783.
36. Lamdan, Y., & Wolfson, H. J. (1988). Geometric hashing: A general and efficient model-based recognition scheme.